数理解析研究所講究録
第 814 巻 1992 年 112-144

A Neural Network Model as a Globally Coupled Map and Applications based on Chaos

野沢 浩 (Hiroshi Nozawa)

Development Div., Nikon Systems Inc.
26-2, Futaba 2-chrome, Shinagawa-ku, Tokyo 140, JAPAN.

(Received)

Abstract

First, a neural network model as the Globally Coupled Map (GCM) is proposed. The model is obtained by modification of a Hopfield network model that has a negative self feedback connection. Secondly, information processed by this model is interpreted in terms of the variety of the maps acting on the network elements, and a new, dynamic information processing model is described. The search for information using vague keywords, and solution of the traveling salesman problem (TSP) are introduced as applications.

1. Introduction

Recently, artificial neural networks based on the high-grade and complicated information processing ability of the brain are being studied and developed. Typical models are the Hopfield network [1] [2], and the back-propagation learning network [3]. These networks consist of very simple single neuron models.

Aihara proposes a chaotic neural network model [4] that comprises a neuron model with chaotic response; this neuron model is a modified Nagumo and Sato neuron model [5]. Tsuda further proposes neural network models that use dynamical systems that have assigned probability being implemented. These models are based on observations of the cerebral cortex column structure [14] [15].

Conversely, Kaneko proposes Globally Coupled Map, GCM systems; GCM systems consist of chaotic elements that are globally coupled. He has investigated their dynamic behavior and information processing ability thoroughly [6]-[10].

We consider a neural network model as one class of GCM system that is composed of single neurons (1-dimensional maps) having a chaotic attractor.

In this paper, first, as the concrete model of the same neural network, we propose a difference model of the Hopfield network that has a negative self feedback connection. Secondly, from a consideration of this model as a GCM, we describe a new, dynamic information processing model that uses single neurons having various attractors. Finally, we introduce two engineering applications using the information processing ability. The applications are the location of information by vague keywords, and solution of the traveling salesman problem (TSP).

2. The neural network model as a GCM

A typical neural network mathematical model is proposed by Hopfield [2]. The model is given by

$$\frac{du_i}{dt} = \sum_{j=1}^{M} T_{ij}v_j - \frac{u_i}{R} + I_i \tag{1}$$

with

$$v_i = g(u_i) = \frac{1}{2}\{1 + \tanh(\frac{u_i}{2\alpha})\}, \tag{2}$$

where, u_i is the input of neuron i (i=1, ..., M) at continuous time t, v_i ($0<v_i<1$) is the output of neuron i, I_i is the threshold value of neuron i, T_{ij} is the synaptic connection of neuron j (j=1, ..., M) to neuron i, R (>0) is the damping constant of the input and α (> 0) is the gain constant of the function g.

If we assume that eq. (1)-(2) has the negative self feedback connection T_{ii} (= -T, T>0), then take the difference equation version of eq. (1)-(2) by Euler's method with the difference step Δt, we obtain a neural network model which is in the form of a GCM. The model is defined by,

$$p_i(n+1) = F_{q_i(n)}\{p_i(n)\}, \tag{3}$$

$$q_i(n) = \frac{1}{T}\{\sum_{j\neq i}^{M} T_{ij}p_j(n) + I_i\} \tag{4}$$

with

$$F_q(p) = rp + (1 - r)[1 - \frac{1}{2}\{1 + \tanh(\frac{p - q}{2\beta})\}], \tag{5}$$

where $p_i(n)$ ($0<p_i(n)<1$) is the internal buffer of neuron i at the discrete time n, the parameter r ($0<r<1$) and β (>0) are given by,

$$r = (1 - \frac{\Delta t}{R}), \tag{8}$$

$$\beta = \frac{\alpha}{RT}. \tag{9}$$

The input and the output of neuron i at the discrete time n are calculated by,

$$u_i(n) = RT\{q_i(n) - p_i(n)\}, \tag{6}$$

$$v_i(n) = g\{u_i(n)\}. \tag{7}$$

This neural network model eq. (3)-(5) is equivalent to the Hopfield network model eq. (1)-(2) with small self feedback connection. It can also be shown to be equivalent to the chaotic neural network proposed by Aihara [4] by a simple variable transformation.

When the synaptic connection T_{ij} is given by $-T\delta_{ij}$ (δ_{ij} is Kronecker's delta.), $q_i(n)$ becomes the following expression:

$$q_i(n) = \frac{I_i}{T} = q_i. \tag{10}$$

From eq. (10), eq. (3) is transformed to the following simple 1-dimensional map:

$$p_i(n+1) = F_{q_i}\{p_i(n)\}, \tag{11}$$

where q_i is the control parameter. Behavior of the single neuron i can be described by this 1-dimensional map eq. (11).

Comparing eq. (3) and (11), and eq. (4) and (10), the model eq. (3)-(5) is recognized to be one class of GCM systems. The characteristic of the class is that the local variable is transformed by a nonlinear map and connected to other variables through the control parameter of the map. That is, in our neural network model eq. (3)-(5) the map $F_{q_i(n)}$ that is a nonlinear transformation from $p_i(n)$ to $p_i(n+1)$ is decided by $p_j(n)$ $(j \neq i)$ at each discrete time n.

3. Behavior of the single neuron i

As previously stated, behavior of the single neuron i is defined by the 1-dimensional map eq. (11). In this section, after discussing the characteristics of eq. (11) as a 1-dimensional map, we shall describe the role of the control parameter q_i in the neural network model eq. (3)-(5).

Figure 1 shows examples of F_{q_i} for a few q_i, and figure 2 shows their trajectories. Figure 3 shows the bifurcation diagram for q_i and the Lyapunov

exponent λ_i.

- Figure 1 -
- Figure 2 -
- Figure 3 -

From figure 1, broadly speaking, we find that the 1-dimensional map F_{q_i} consists of two parallel, positive slope straight lines,

$$p_i(n+1) = rp_i(n) + (1 - r), \tag{12}$$
$$p_i(n+1) = rp_i(n), \tag{13}$$

and a negative slope curved line interpolating these lines. The slope r of eq. (12) and (13) is between 0 and 1. The curved line has a local slope of less than -1 at the midpoint which is at $(q_i, rq_i + (1 - r)/2)$.

It is clear from the definition of the Lyapunov exponent, that when the trajectory of $p_i(n)$ is generated solely by the map eq. (12) and (13), it is not chaotic behavior (see figure 2 a, c, d, f and g). When the straight and the curved lines are used as the map, however, the trajectory of $p_i(n)$ can be chaotic (see figure 2 b and e). The map F_{q_i} can generate a chaotic trajectory of $p_i(n)$ due to the above-mentioned negative slope curved line.

The parameter q_i controls the position of this curved line on the coordinate axis $p_i(n)$. Therefore, the behavior of $p_i(n)$ becomes chaotic, periodic and fixed according to the value of q_i (see figure 3). Table 1 shows the character of F_{q_i} for different ranges of q_i.

- Table 1 -

Here, we can estimate the behavior of each neuron i in the model eq. (3)-(5) with figure 1-3. We can therefore deduce the next fact.

In the case of the single neuron i, F_{q_i} is a map independent of time. So F_{q_i} causes only one nonlinear transformation. However, since map $F_{q_i(n)}$ is changes with time in the neural network, it is possible that $F_{q_i(n)}$ induces various nonlinear transformations (for example, figure 1 a at the time n, figure 1 b at the time n+1 and so on). Namely, since the single neuron i connects with other neurons j, F_{q_i} changes to various maps $F_{q_i(n)}$.

We have found the meaning of the connection (the neural network) at this point. Now, we can propose a new information processing model using the variety of $F_{q_i(n)}$.

4. Behavior of the neural network

As described in the section 3., the meaning of the neural network model eq. (3)-(5) as the GCM lies in the variety of maps $F_{q_i(n)}$.

In this section, after discussing the way CAM (Content-Addressable Memory), proposed by Hopfield, [1] [2] uses just two types of the various maps $F_{q_i(n)}$, we shall describe a dynamic information processing model that uses a greater variety (fixed, periodic and chaotic) of maps $F_{q_i(n)}$.

4.1. The variety of maps $F_{q_i(n)}$ in the CAM

Suppose that the synaptic connection T_{ij} is symmetric ($T_{ij} = T_{ji}$) and the self feedback connection T_{ii} is zero ($T_{ii} = 0$). Hopfield shows that in this case the model eq. (1)-(2) behaves in such a way that the energy function decreases [2]. The energy function is defined by

$$E = -\frac{1}{2}\sum_{i=1}^{M}\sum_{j=1}^{M} T_{ij}v_iv_j - \sum_{i=1}^{M} I_iv_i + \frac{1}{R}\sum_{i=1}^{M}\int_{\frac{1}{2}}^{v_i} g^{-1}(v)dv \quad , \tag{14}$$

where, the synaptic connection T_{ij} is given by the following method with the vector patterns V^s (= $\{V^s_1, ..., V^s_M\}$, s = 1, ..., N):

$$T_{ij} = \sum_{s=1}^{N} (2V^s_i - 1)(2V^s_j - 1) \quad . \tag{15}$$

From eq. (15), each vector pattern V^s can correspond to a minimum value of the energy function eq. (14) [1]. Hopfield proposed that the model eq. (1) and (2) be used for the associated memory by regarding each vector pattern V^s as the content of memory. He named the information processing model CAM.

Our neural network model eq. (3)-(5) can achieve CAM by using a small self feedback connection. Then, how does the action of the variety of maps $F_{q_i(n)}$ decide the trajectory of $p_i(n)$ at the discrete time n.

- Figure 4 -

For the purpose of simulation, we construct the model eq. (3)-(5) of M = 16 neurons that are defined by the 1-dimensional map eq. (11). The synaptic connection T_{ij} is decided by eq. (15) with three orthogonal vector patterns (see

figure 4). Now we shall investigate the behavior of the model eq. (3)-(5) that has the small self feedback connection T (=1).

Figure 5 shows the trajectories of the internal buffer $p_2(n)$ and $p_8(n)$. Figure 6 shows that the maps $F_{q_2(n)}$ and $F_{q_8(n)}$ (n = 1, ..., 4) decide their trajectories. Figure 7 shows how the behavior of q(n) (= $\{q_1(n), ..., q_M(n)\}$) decides the variety of $F_{q_i(n)}$.

- Figure 5 -
- Figure 6 -
- Figure 7 -

From figure 5-7, in the case of recall of the vector pattern F, $F_{q_{i1}(n)}$ (i1 = 2, 3, 4, 5, 9, 10, 11, 13) converges to a map that is approximated by eq. (12) at the time n (= 4):

$$p_i(n+1) \sim rp_i(n) + (1 - r), \tag{16}$$

and the trajectory of $p_{i1}(n)$ is driven into 1. Also, $F_{q_{i0}(n)}$ (i0 = 1, 6, 7, 8, 12, 14, 15, 16) converges to a map that is approximated by eq. (13) at the time n (=1):

$$p_i(n+1) \sim rp_i(n), \tag{17}$$

and the trajectory of $p_{i0}(n)$ is driven into 0.

The reason why the variety of $F_{q_i(n)}$ are described by just eq. (16) and (17) is that the self feedback connection T is small in eq. (4). The variable $q_i(n)$ goes out of the region ($0 < q_i(n) < 1$) that has the variety of $F_{q_i(n)}$ (see figure 7).

4.2. Dynamic information processing model using the variety of maps $F_{q_i(n)}$

As explained in 4.1, we can interpret the CAM as a skillful information processing model using just two maps eq. (16) and (17) in the variety of maps $F_{q_i(n)}$.

Here, we propose a dynamic information processing model that uses a greater variety of maps.

First, when $p_i(n)$ is transformed by the 1-dimensional map F_{q_i} eq. (11), we put the control parameter q_i to the following expression:

$$q_i = \frac{I_i}{T} = 0.09 \quad . \tag{18}$$

Then, we can set $p_i(n)$ to the chaotic behavior (figure 2 b) independent of the self

feedback connection T.

Secondly, we construct the model eq. (3)-(5) that has the synaptic connection T_{ij}. The synaptic connection T_{ij} is defined by eq. (15) with three orthogonal vector patterns C, F and 4.

Finally, we need a method to determine the self feedback connection T. The self feedback connection T is chosen in such a way that variable $q_i(n)$ exists between 0 and 1.

Generally, the vector pattern which is recalled by the model eq. (3)-(5) at the discrete time n is recognized by the output $v_i(n)$ of neuron i. The output is calculated by eq. (6)-(7) [2] [4]. In contrast to this, we recognize the vector pattern by the variable $q_i(n)$ that decides the variety of $F_{q_i(n)}$. Our focus is not the actual activity $v_i(n)$ but the virtual activity $q_i(n)$, namely, the variety of nonlinear transformations. If we take small self feedback connection, the actual activity $v_i(n)$ just obeys the virtual activity $q_i(n)$.

The vector patterns C, F and 4 that are stored as the memory have a characteristic structure; the structure is that there are equal numbers of 1 and 0.

From now on, the vector pattern $\phi(n)$ $(= \{\phi_1(n), \ldots, \phi_M(n)\})$ that is recalled by the model eq. (3)-(5) in the virtual level is obtained by dividing the variety of $F_{q_i(n)}$ into two, equal parts. The method of division is the following simple coding using the mean of $q_i(n)$:

$$\phi(n) = \begin{cases} q_i(n) \geq \bar{q} \rightarrow 1, \\ q_i(n) < \bar{q} \rightarrow 0 \end{cases} \tag{19}$$

with

$$\bar{q} = \lim_{n\to\infty} \frac{1}{nM} \sum_{k=0}^{n-1} \sum_{i=1}^{M} q_i(k) \quad . \tag{20}$$

Figure 8 shows the Lyapunov spectrum λ $(=\{\lambda_1, \ldots, \lambda_M\})$ [11] for a range of values of the self feedback connection T $(10 < T < 21)$.

- Figure 8 -

From figure 8, the Lyapunov spectra that have positive maximal Lyapunov exponent are classified into three types. The three types are the following (a)-(c):

(a) large flat structure
(b) smooth continuous structure
(c) partially flat structure

Next, we select typical values of T corresponding to types (a)-(c) and study the

behavior of the model eq. (3)-(5) there.

(a) large flat structure (T=13.1)

Figure 9 shows behavior of variable $q(n) = \{q_1(n), ..., q_M(n)\}$ (we call these Kaneko plots [6]~ [8].), the vector pattern $\phi(n) = \{\phi_1(n), ..., \phi_M(n)\}$ that is recalled in the virtual level and the precision ($1/p = 10^{-4}$) dependent cluster number $k^p(n)$ [7] that means the effective degrees of freedom for q(n).

- Figure 9 -

In figure 9, the variable q(n) is separated into two groups and has almost periodic oscillation (maximal Lyapunov exponent $\lambda_1 \sim 0.2$, Lyapunov dimension [12] $D\lambda \sim 6$).

Thus, the variety of $F_{q_i(n)}$ is classified into two types, the vector pattern $\phi(n)$ becomes only vector pattern F and the cluster number $k^p(n)$ takes the constant value (= 8) independent of the time n.

Many other attractors that recall other vector patterns (C, 4 and so on) are obtained with different initial condition $p(0) = \{p_1(0), ..., p_M(0)\}$. However, their behavior is similar.

(b) smooth continuous structure (T=15)

Figure 10 shows behavior of q(n), $\phi(n)$ and $k^p(n)$.

- Figure 10 -

In figure 10, the variable q(n) separates into various groups, almost merge again to one group and then separates again into other groups, and so on repeatedly. The behavior is complicated and irregular (maximal Lyapunov exponent $\lambda_1 \sim 0.5$, Lyapunov dimension $D\lambda \sim 15$).

As the result, the $F_{q_i(n)}$ has innumerable types that are decided by chaotic trajectory of $q_i(n)$, in the variety of $F_{q_i(n)}$ is generated by chaos, the vector pattern $\phi(n)$ becomes a nonperiodic time series visiting all patterns C, F, 4, C, F, 4 (_is reversed pattern) and the cluster number $k^p(n)$, nonperiodic, fluctuates between about 9 degrees of freedom, and about 13 degrees of freedom.

Although changing initial condition p(0), dose not change the fact that all patterns are recalled in a nonperiodic time series, we find there are many attractors that have a different recall-frequency of each vector pattern.

(c) partially flat structure (T=17.2)

Figure 11 shows behavior of q(n), ϕ(n) and k^p(n).

- Figure 11 -

In figure 11, the variable q(n) is almost periodic in the way that it repeatedly merges almost into one group only to separate again into various groups (maximal Lyapunov exponent $\lambda_1 \sim 0.2$, Lyapunov dimension $D_\lambda \sim 7$).

The variety of $F_{q_i(n)}$ is classified into six types, the vector pattern ϕ(n) becomes the periodic time series visiting C, 4, and F, and the cluster number k^p(n) takes the constant value (= 9) almost independent of the time n.

With change the initial condition p(0) we find many attractors that have different periods and recall patterns.

We have described the dynamic behavior of the model eq. (3)-(5) for the typical three values of self feedback connection T. In particular, behavior of case (b) may be related with "Chaotic Itinerancy" [6] [13] [14] [15], an expected universal phenomenon in chaotic dynamical systems that have a great deal of freedom.

5. Applications for the dynamic information processing model

The dynamic information processing model, is network model eq. (3)-(5) plus the coding and parameter selection described in section 4, has various information processing abilities due to the use of the variety of maps $F_{q_i(n)}$. In this section, we introduce two concrete, applied examples as follows:

(a) the search for information using vague keywords,
(b) solution of the TSP.

5.1. The search for information using vague keywords

The information (reference information) memorized in the database of a computer is searched for by the input of associated keywords. When we search for the information, the associated keywords must be specific. The more information there is stored in the database, the more detailed the keyword instructions need be. The procedures which specify these keywords become increasingly difficult.

Conversely, if the access information is vague, it is difficult to specify keywords adequately. Suppose one inputs a wrong keyword, reference systems that are not user-friendly say "nothing" in the worst case, although information exists within the system.

The search for information using vague keywords, using the information processing ability of the model eq. (3)-(5) aims to solve the two difficult problems mentioned above. A search procedure using an optical system with chaos also has been reported [16].

We set behavior of the model eq. (3)-(5) to the situation in 4.2. (b). Here the reference information is six vector patterns (C, F, 4, C, F, 4).

The keywords k (= {k1, ..., kM}) are input by control parameter q_i eq. (18) as follows:

$$q_i = \frac{I_i}{T} = \begin{cases} 0.08 \rightarrow k_i = 0\,, \\ 0.09 \rightarrow k_i = \text{"nothing"}, \\ 0.10 \rightarrow k_i = 1 \end{cases} \tag{21}$$

From eq. (21), the model eq. (3)-(5) behaves like 4.2. (b) under conditions that no keywords k are input.

We investigate behavior of the model eq. (3)-(5) when keywords k are input. Figure 12 shows two keywords k that have been input. Figure 13 shows behavior of the variable q(n) and the vector pattern $\phi(n)$.

- Figure 12 -
- Figure 13 -

When the vector pattern C is given as keyword, the variable q(n) behaves similar to 4.2. (a) and the vector pattern $\phi(n)$ becomes C only (maximal Lyapunov exponent $\lambda_1 \sim -0.2$).

In this case, when keyword k is given, the model eq. (3)-(5) switches from chaotically moving around all the information, to outputting necessary information only (chaotic search process). Therefore, the model eq. (3)-(5) has the ability to search for information. This behavior is similar to that observed in experiments by Freeman [17] .

When we input the keyword k that is two Hamming distances away from the information C, the variable q(n) behaves similar to 4.2. (b) and the vector pattern $\phi(n)$ visits all stored patterns (maximal Lyapunov exponent $\lambda_1 \sim 0.3$, Lyapunov dimension $D_\lambda \sim 13$).

We notice though that information C is recalled the most. It shows that the information C has the shortest Hamming distance to the keyword k. When we input keywords k, corresponding to patterns which are not stored in the network unhelpful reference systems say "nothing". However, this model switches to chaotic search and the information closest to the keywords k is recalled most

frequently. As a result, we obtain substitute information.

We investigated situations where one keyword k is given that has the same Hamming distance to information C and F, and we obtained the result that C and F are recalled the most frequently.

In this section we showed examples of search for information using vague keywords. Although they are on a very small scale, for the total information amounts to only six pieces, the search ability of the model eq. (3)-(5) is expected to solve the two information access problems mentioned at the beginning of the section.

5.2. Solution of the TSP

The TSP is defined as the task of the salesman visiting all the N cities on his list once and once only, and returning to his starting point after traveling the minimum possible distance. That is a classic combinatorial optimization problem (NP complete).

Hopfield proposes a solution with high speed and good approximate accuracy for the TSP using the model eq. (1)-(2), and he shows an example solution using a concrete number N (= 10) of city coordinate values. We can also solve the TSP by the model eq. (3)-(5).

First of all, the expression for the solution of the TSP uses the same method proposed by Hopfield (neurons arranged in N×N grid patterns, the visiting order N indicated by lateral position, the city names N indicated by longitudinal position, so each neuron is expressed by the suffix of city name i, j = 1, ..., N and the suffix of visiting order k, l = 1, ..., N).

Next, after this expression, the estimation function E(n) is decided by the constraint term $E_1(n)$ and the total path length term $E_2(n)$ as follows:

$$E(n) = \frac{1}{2}\{AE_1(n) + BE_2(n)\}, \tag{22}$$

where A and B are positive constants, the constraint term $E_1(n)$ is defined by,

$$E_1(n) = \sum_{i=1}^{N}\{\sum_{k=1}^{N} v_{ik}(n) - 1\}^2 + \sum_{k=1}^{N}\{\sum_{i=1}^{N} v_{ik}(n) - 1\}^2, \tag{23}$$

and the total path length term $E_2(n)$,

$$E_2(n) = \sum_{i=1}^{N}\sum_{j=1}^{N}\sum_{k=1}^{N} d_{ij}v_{ik}(n)\{v_{jk+1}(n) + v_{jk-1}(n)\}, \tag{24}$$

where $v_{ik}(n)$ is the output of each neuron ik at the discrete time n, d_{ij} is the constant value of distance from the city j to i, $v_{i0}(n)=v_{iN}(n)$ and $v_{iN+1}(n)=v_{i1}(n)$.

From eq. (22)-(24), the synaptic connection T_{ikjl} and the threshold value I_{ik} of the model eq. (3)-(5) to solve for the TSP are decided by,

$$T_{ikjl} = - A\{\delta_{ij}(1 - \delta_{kl}) + \delta_{kl}(1 - \delta_{ij})\} - Bd_{ij}(\delta_{lk+1} + \delta_{lk-1}), \tag{25}$$

$$I_{ik} = A. \tag{26}$$

We solve the TSP of N = 10 cities by controlling the self feedback connection T by the model eq. (3)-(5) that is composed of M = 100 neurons.

The city coordinate values use Hopfield's original data [19] (see figure 14). The constant values A and B are both 1 in eq. (25) and (26).

The solution for the TSP is obtained from the following vector pattern $\phi(n)$ $(= \{\phi_{11}(n), ..., \phi_{NN}(n)\})$ that is recalled in the virtual level:

$$\phi_{ik}(n) = \begin{cases} q_{ik}(n) \geq \tilde{q}(n) \rightarrow 1, \\ q_{ik}(n) < \tilde{q}(n) \rightarrow 0, \end{cases} \tag{27}$$

where $\tilde{q}(n)$ is the tenth value of $q_{ik}(n)$ in order of decreasing size at each time n.

Figure 14 shows city coordinate values and the best three routes of travel. Figure 15 shows the solution abilities of the Hopfield model eq. (1)-(2) (using the method of slowly increasing the gain constant to get the best performance) and the model eq. (3)-(5) (T=1.3).

Here, the initial condition p(0) $(= \{p_{11}(0), ..., p_{NN}(0)\})$ is chosen by independent random numbers, so that the constraint term eq. (23) becomes 0. The cut off time for solution is 1000.

- Figure 14 -
- Figure 15 -

Each circle graph in figure 15 shows the recall-frequency of the best route, the second, the third, and other good routes and the bad routes (eq. (22)$\neq$0) obtained with 1000 different initial conditions p(0). The model eq (3)-(5) always visits the best route within 200$\sim$300 steps. Clearly, the solution ability of the model eq (3)-(5) is better than eq. (1)-(2).

Figure 16 shows behavior of the variable q(n) and the estimation function E(n) with the vector pattern $\phi_{ik}(n)$ substituted for the output $v_{ik}(n)$ in eq. (23) when the best route is recalled by the model eq. (3)-(5).

- Figure 16 -

In figure 16, the search for the solution of the TSP is divided into two processes, one is transient search by strong chaotic state ($D\lambda \sim 10$), the other is recall by weak chaotic state ($D\lambda \sim 3$).

This is similar to the behavior of the model eq. (3)-(5) on conditions that the correct keywords are input in 5.1. This is a characteristic of the model eq. (3)-(5) when it is applied to solution of the TSP.

6. Summary and Discussion

After we supposed that the Hopfield network model eq. (1)-(2) has a negative self feedback connection, and took the difference equation version of eq (1)-(2) by Euler's method, we obtained the neural network model eq. (3)-(5) as one class of the GCM.

The characteristic of the model eq. (3)-(5) as a GCM is that the local variable (we call it the internal buffer of a neuron) is transformed by a nonlinear map that connects to other neurons through the control parameter eq. (10) of the map.

One-dimensional maps eq. (11) that describe the behavior of the single neuron were investigated for their dependence on the control parameter eq. (10). The map eq. (11) has many kinds of attractors (fixed points, periodic and chaotic) when the parameter eq. (10) exists between 0 and 1.

As a result, information can be processed by the model eq. (3)-(5) using a variety of maps (network elements).

From this point of view, first of all, we investigate the CAM. The CAM can be interpreted as a information processing model which uses just two maps eq. (16) and (17) in the variety of maps.

Next, we propose a dynamic processing model that uses a greater variety of maps and we investigate dynamic behavior of the model eq. (3)-(5). The dynamic behavior (information processing ability) of the model eq. (3)-(5) is classified into the following:

(a) recall of only one stored memory in the weak chaos state,
(b) all stored memories are recalled nonperiodically in the strong chaos state,
(c) some stored memories are recalled periodically in the chaos between (a) and (b).

This information processing ability (a)-(c) can be classified by the structure of Lyapunov spectrum.

Finally, two examples of engineering applications are shown as follows:

(d) the search for information using vague keywords,
(e) solution of the traveling salesman problem.

The ability of the model eq. (3)-(5) is better than eq. (1)-(2) for both (d) and (e). From this result, we can interpret that the complexity of the problems are overcome by the variety of maps.

One class in the GCM systems (for example our neural network model) is expected to be applicable to many information processes on condition that the elements of GCM have various attractors. We have to consider how to quantity properties such as "variety of maps" in order to evaluate the quantities which characterize dynamic behavior in the GCM and which can be used to estimate performance in these applications.

The control parameter of the maps in our neural network model can be driven by chaotic trajectory (4.2. (b)). This approach should be compared and contrasted the dynamical system [14] [15] [20] that has a countable number of map control parameters which are chosen with certain probabilities.

Acknowledgments

The author would like to thank I. Shimada, K. Kaneko, I. Tsuda, Y. Iba and K. Aihara for useful discussions. He also would like to thank Nikon Corporation, Nikon Systems Inc., Fujitsu Corporation, H. Abe, K. Kadowaki, K. Yamazaki, H. Yamaguchi and E. Nozawa for useful supports.

References

[1] J.J. Hopfield, Proc. Natl. Acad.Sci.USA 79 (1982) 2554.
[2] J.J. Hopfield, Proc. Natl. Acad.Sci.USA 81(1984) 3088.
[3] D. E. Rumelhart, G. E. Hinton and R. J. Williams, Nature 323 (1986) 533.
[4] K. Aihara, T. Takabe and M. Toyoda, Phys. Lett. A 144 (1990) 333
[5] J. Nagumo and S. Sato, Kybernetic 10 (1972) 155.
[6] K. Kaneko, Physica D 41(1990)137.
[7] K. Kaneko, Physica D 54 (1991) 5.
[8] K. Kaneko, Phys. Rev. Lett. A 144 (1990)333.
[9] K.Kaneko, J. Phys. A24 (1991) 2107.
[10] K. Kaneko, Phys. Rev. Lett.65 (1990)1391.
[11] I. Shimada and T. Nagashima, Prog. Theor. Phys. 61 (1979) 1605.
[12] J. P. Eckmann and D. Ruelle, Rev. Mod. Phys.57 (1985) 617
[13] K. Ikeda, K. Matsumoto and K. Ohtsuka, Prog. Theor. Phys. Suppl. 99 (1989) 295.
[14] I. Tsuda, in: Neurocomputers and Attention: Neurobiology, synchronization

and chaos, eds. A.V.Holden and V.I.Kryukov (Manchester Univ. Press, 1991).
[15] I.Tsuda,Neural Networks 5 (1992)313.
[16] P. Davis, Jap. J.Appl. Phys. 29 (1990) L1238.
[17] W. Freeman and C. A. Skarda, Brain Res.Rev.10 (1985)147.
[18] J. J. Hopfield and D. W. Tank, Biol.Cybern. 52 (1985) 52.
[19] G. V. Wilson and G. S. Pawley, Biol. Cybern. 58 (1988) 63.
[20] M. Barnsley, Computer Graphics 22 (1988) 131.

Figure captions

Figure 1 : Examples of 1 dimensional map F_{q_i} ($r = 0.7$, $\beta = 0.006$) for a few q_i is shown. The thick line shows F_{q_i}. Two parallel dashed dotted lines show 1-dimensional map eq. (12) and (13). The dashed line drawn at a slant shows $p_i(n+1) = p_i(n)$. The vertical dotted line shows $p_i(n) = q_i$. (a) $q_i = 0.0$, (b) $q_i = 0.09$, (c) $q_i = 0.25$, (d) $q_i = 0.5$, (e) $q_i = 0.65$, (f) $q_i = 0.85$, (g) $q_i = 1.0$.

Figure 2 : Trajectories about fig. 1 (a)-(g) are shown. The fine line shows trajectory. (a) Transient trajectory to fixed point (-0.0226), $\lambda_i = -0.9047$. (b)Chaotic trajectory, $\lambda_i = 0.4042$. (c) 3 periodic trajectory, $\lambda_i = -0.6910$. (d) 2 periodic trajectory, $\lambda_i = 0.3567$. (e) Chaotic trajectory, $\lambda_i = 0.3660$. (f) 4 periodic trajectory, $\lambda_i = -0.2649$. (g) Transient trajectory to fixed point (0.9774), $\lambda_i = -0.9047$.

Figure 3 : (a) Bifurcation diagram of 1-dimensional map F_{q_i} ($r = 0.7$, $\beta = 0.006$) for q_i is shown. Two parallel dashed dotted lines show $p_i(n) = rq_i + (1 - r)$ and $p_i(n) = rq_i$. (b) The Lyapunov exponent λ_i of 1-dimensional map F_{q_i} for q_i is shown. The dashed line shows $\lambda_i = 0$.

Figure.4 : Vector patterns stored in the neural network as the memory are shown. The white square shows $v_i = 0$ and the black squares shows $v_i = 1$. (a) The arrangement of neuron index i (=1, ..., 16), (b) Vector pattern C. (c) Vector pattern F. (d) Vector pattern 4.

Figure 5 : Trajectories of the internal buffer during recall of the vector pattern F are shown ($r = 0.7$, $\beta = 0.006$). (a) Transient trajectory of neuron 2 to local fixed point (~ 1). (b) Transient trajectory of neuron 8 to local fixed point (~ 0).

Figure 6 : Maps $F_{q_2(n)}$ and $F_{q_8(n)}$ ($n = 0, ..., 3$) deciding fig.5 (a)-(b) are shown. The thick line shows $F_{q_i(n)}$. Two parallel dashed dotted lines show eq. (12) and (13). The dashed line drawn at a slant shows $p_i(n+1) = p_i(n)$. (a) $F_{q_2(0)}$, (b) $F_{q_2(1)}$, (c) $F_{q_2(2)}$, (d) $F_{q_2(3)}$, (e) $F_{q_8(0)}$, (f) $F_{q_8(1)}$, (g) $F_{q_8(2)}$, (h) $F_{q_8(3)}$.

Figure 7 : Behavior of variable q(n) (= {$q_1(n)$, ..., q_M (n)}, n = 0, ..., 50) deciding the variety of $F_{q_i(n)}$ (r = 0.7, β = 0.006) is shown. The continuous lines show $q_{i1}(n)$ (i1 = 2, 3, 4, 5, 9, 10, 13). The dashed lines show $q_{i0}(n)$ (i0 = 1, 6, 7, 8, 12, 14, 15, 16).

Figure 8 : Structure of Lyapunov spectrum λ (= {λ_1, ..., λ_{16}}) for a range of the self feedback connection T ($10 \leqq T \leqq 21$) is shown (r = 0.7, β = 0.006). (a) Large flat structure. (b) Smooth continuous structure. (c) Partially flat structure.

Figure 9 : Behavior of the variable q(n), the vector pattern ϕ(n) and the cluster number $k^p(n)$ in the region fig.8 (a) (T = 13.1) are shown (r = 0.7, β = 0.006). (a) q(n), (b) ϕ(n) (the symbol O means "other" (not memory) patterns), (c) $k^p(n)$, n = 100000, ..., 100200.

Figure 10 : Behavior of the variable q(n), the vector pattern ϕ(n) and the cluster number $k^p(n)$ in the region fig.8 (b) (T = 15) are shown (r = 0.7, β = 0.006). (a) q(n), (b) ϕ(n) (the symbol O means "other" (not memory) patterns), (c) $k^p(n)$, n = 100000, ..., 100200.

Figure 11 : Behavior of the variable q(n), the vector pattern ϕ(n) and the cluster number $k^p(n)$ in the region fig.8 (c) (T = 17.2) are shown (r = 0.7, β = 0.006). (a) q(n), (b) ϕ(n) (the symbol O means "other" (not memory) patterns), (c) $k^p(n)$, n = 100000, ..., 100200.

Figure 12 : Two keywords k input to the model eq. (3)-(5) are shown. The white square shows k_i = 0 and the black square shows k_i = 1. (a) The keyword C. (b) A keyword which is two Hamming distances away from the keyword C.

Figure 13 : Behavior of the variable q(n) and the vector pattern ϕ(n) resulting from input of keywords k are shown (r = 0.7, β = 0.006). (a) q(n), (c) ϕ(n) (n = 100000, ..., 100200) with the keyword fig.12 (a). (b) q(n), (d) ϕ(n) (n = 100000, ..., 100200) with the keyword fig.12 (b).

Figure 14 : (a) 10 city (A - J) coordinate values [19] are shown. (b) Best route. (c) Second best route. (d) Third best route.

Figure 15 : (a) Solution abilities of the model eq. (1)-(2) and eq. (3)-(5) for the TSP are shown (r = 0.7, β = 0.006). (a) Ability of the model eq. (1)-(2) (best =14.3%, second = 5.5%, third = 1.1%, other = 78.8% and bad = 0.3%). (b)

Ability of the model eq. (3)-(5) (best = 94.7%, second = 2.5%, third = 0.5%, other = 2.1% and bad = 0.2%).

Figure 16 : Behavior of the variable q(n) and the energy function E(n) for ϕ(n) are shown (r = 0.7, β = 0.006). (a) q(n), (b) E(n), n = 1760, ..., 1960.

Table 1

Character of 1-dimensional map F_{q_i} (r = 0.7, β = 0.006) for the rough range of control parameter q_i.

range of q_i	Character of 1-dimensional map F_{q_i}
$q_i < 0$	Having only Fixed point attractors (~0)
$0 \leqq q_i \leqq 1$	Having various Fixed point, periodic and chaotic attractors
$q_i > 1$	Having only Fixed point attractors (~1)

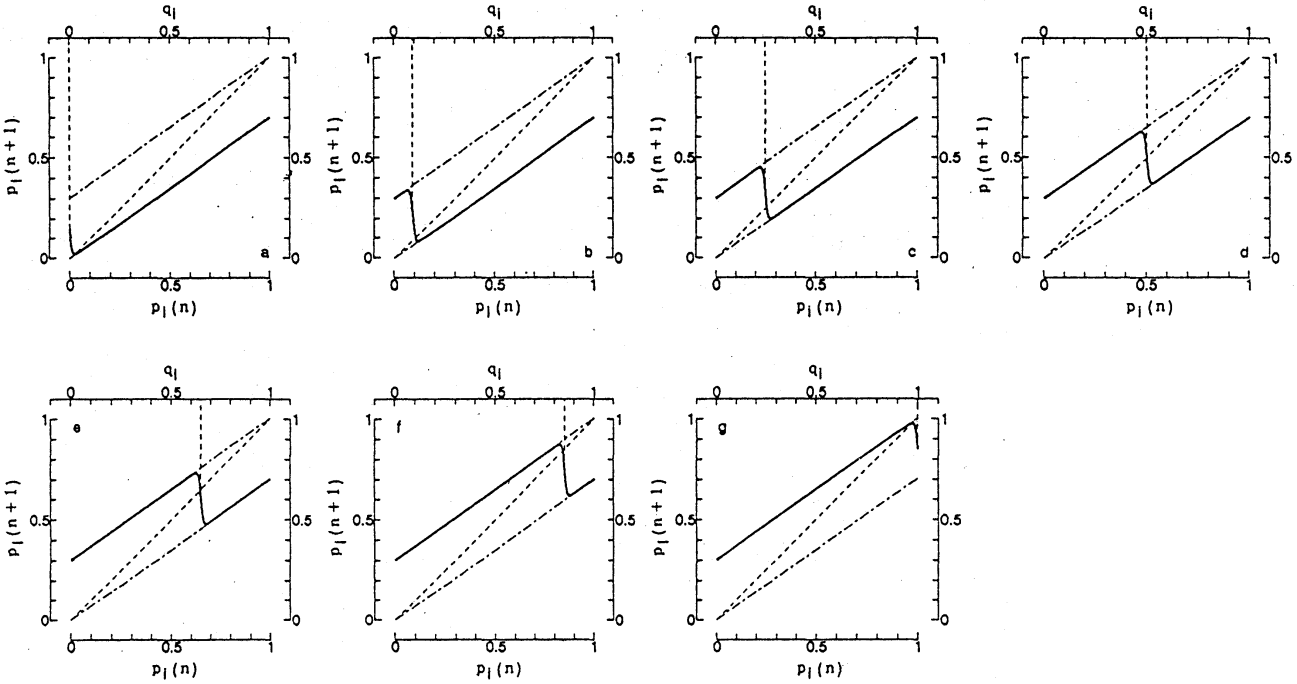

Nozawa Figure 1

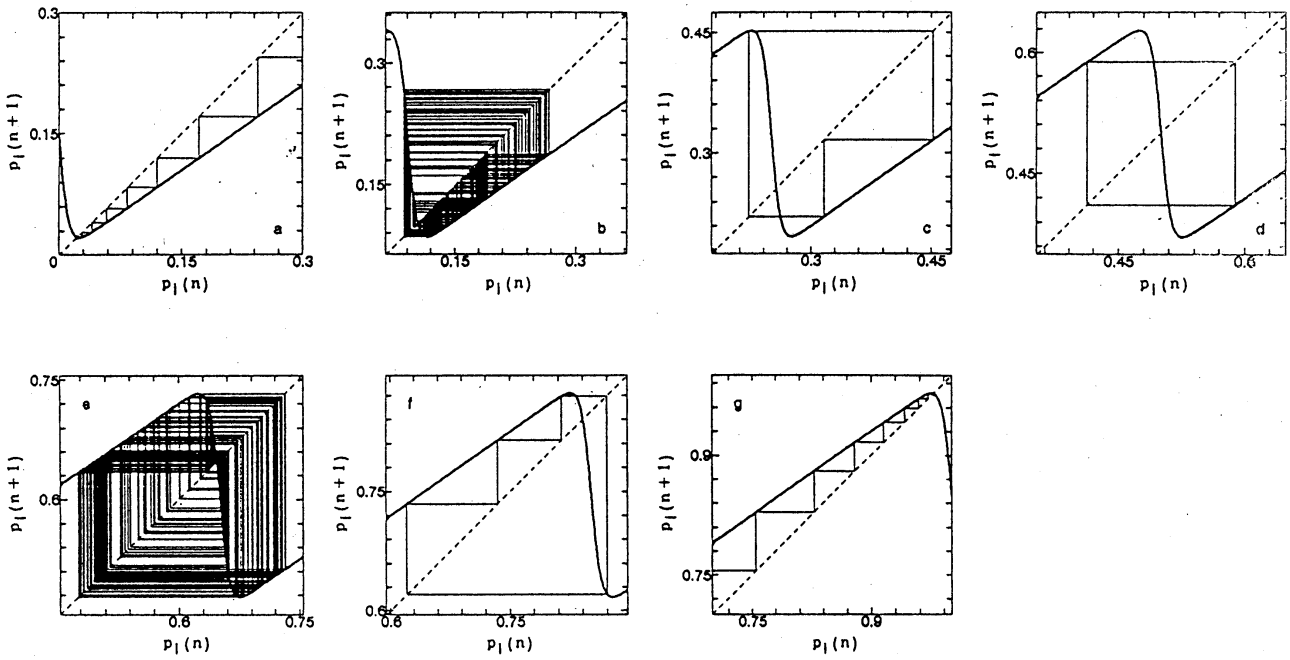

Nozawa Figure 2

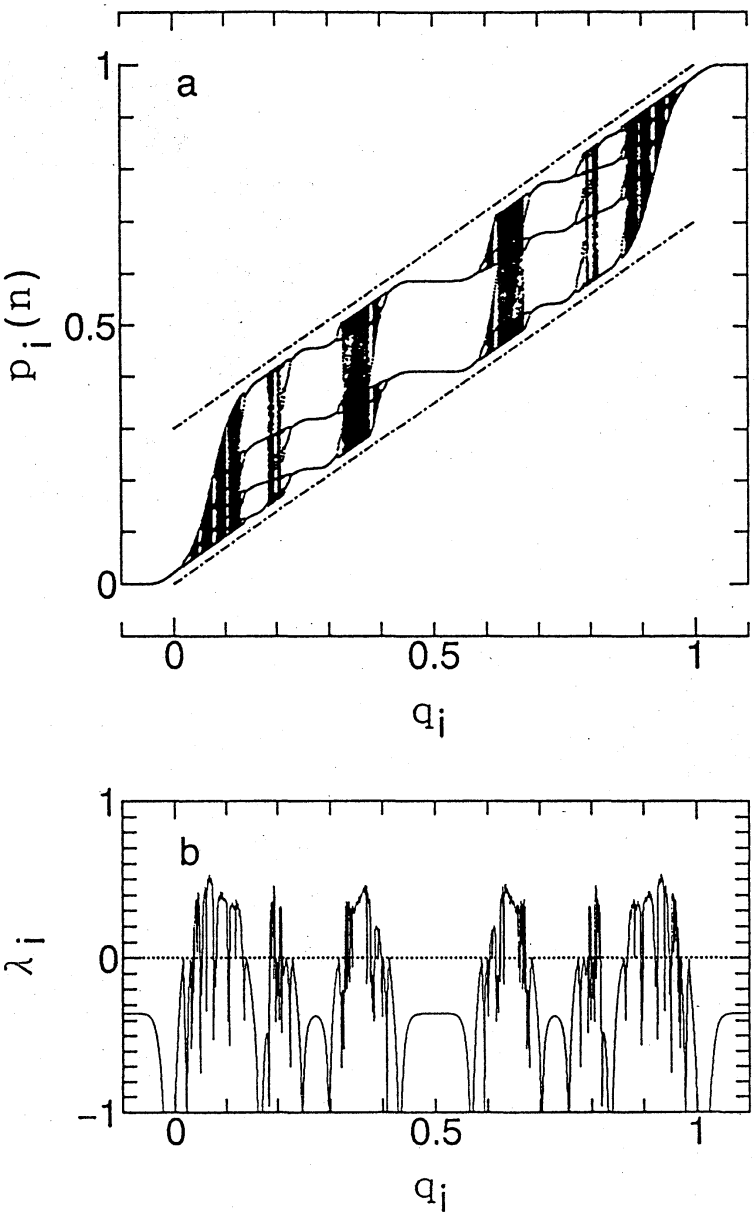

Nozawa Figure 3

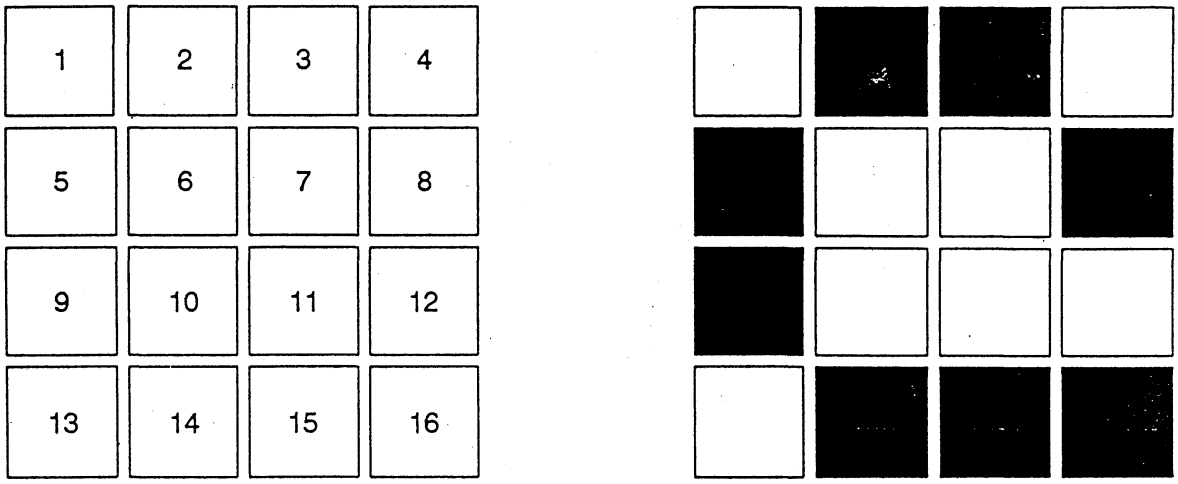

a b

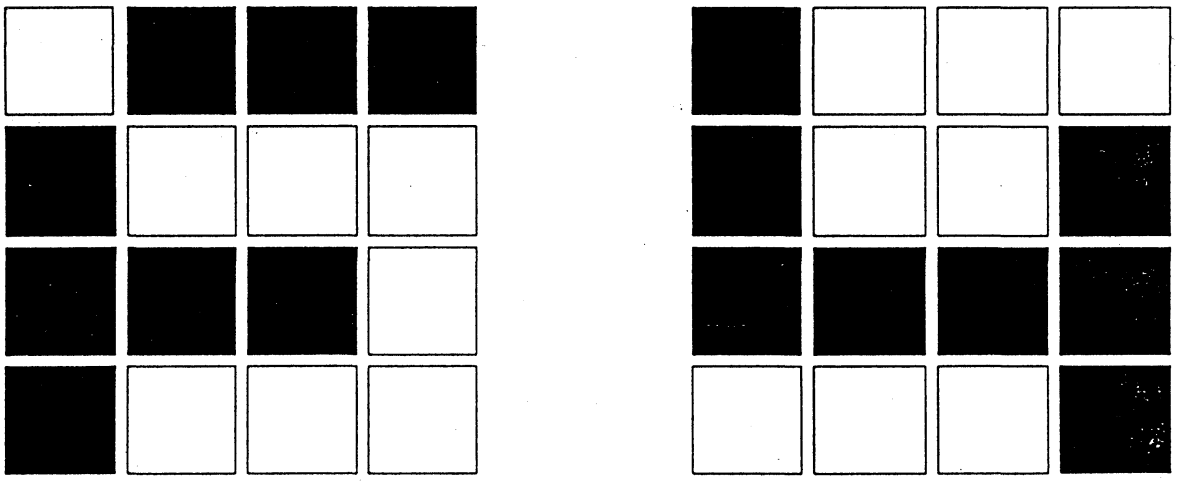

c d

Nozawa Figure 4

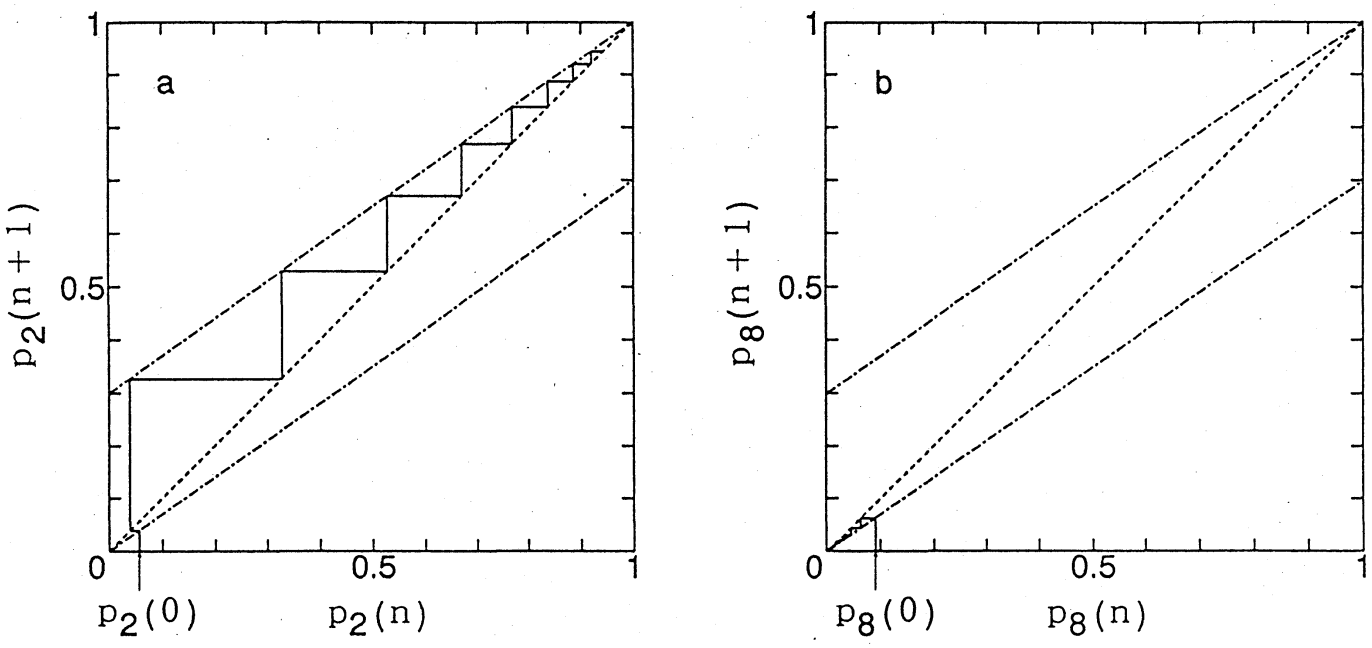

Nozawa Figure 5

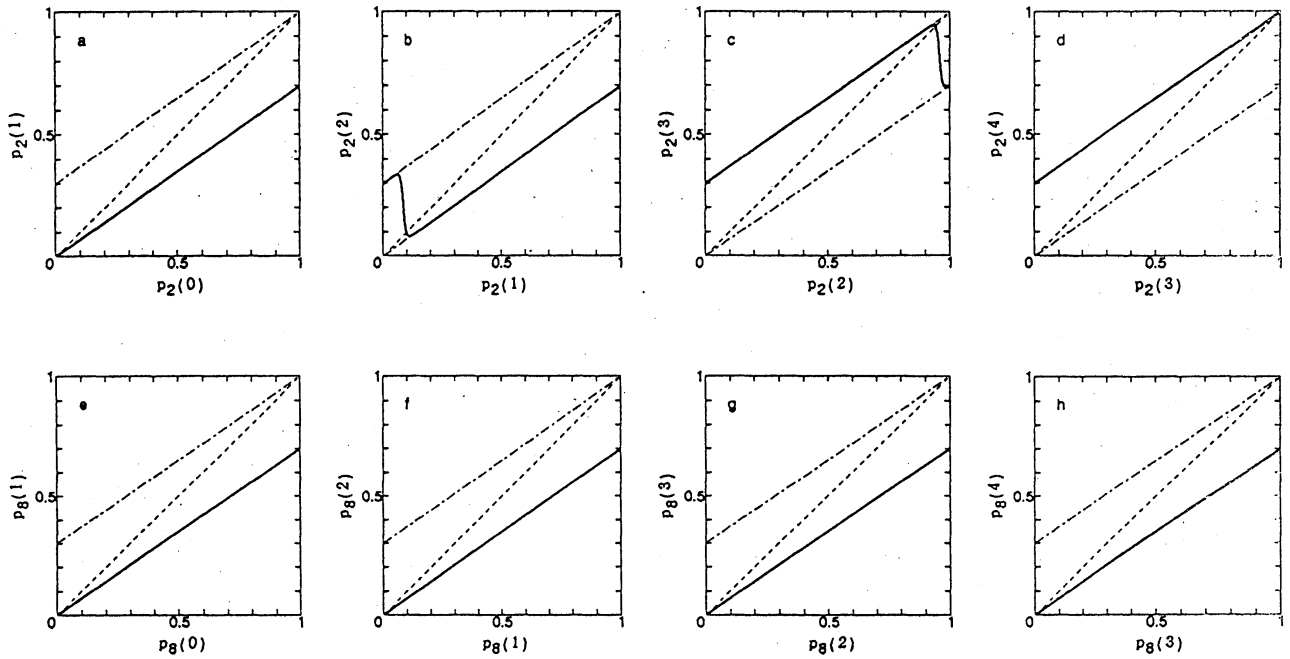

Nozawa Figure 6

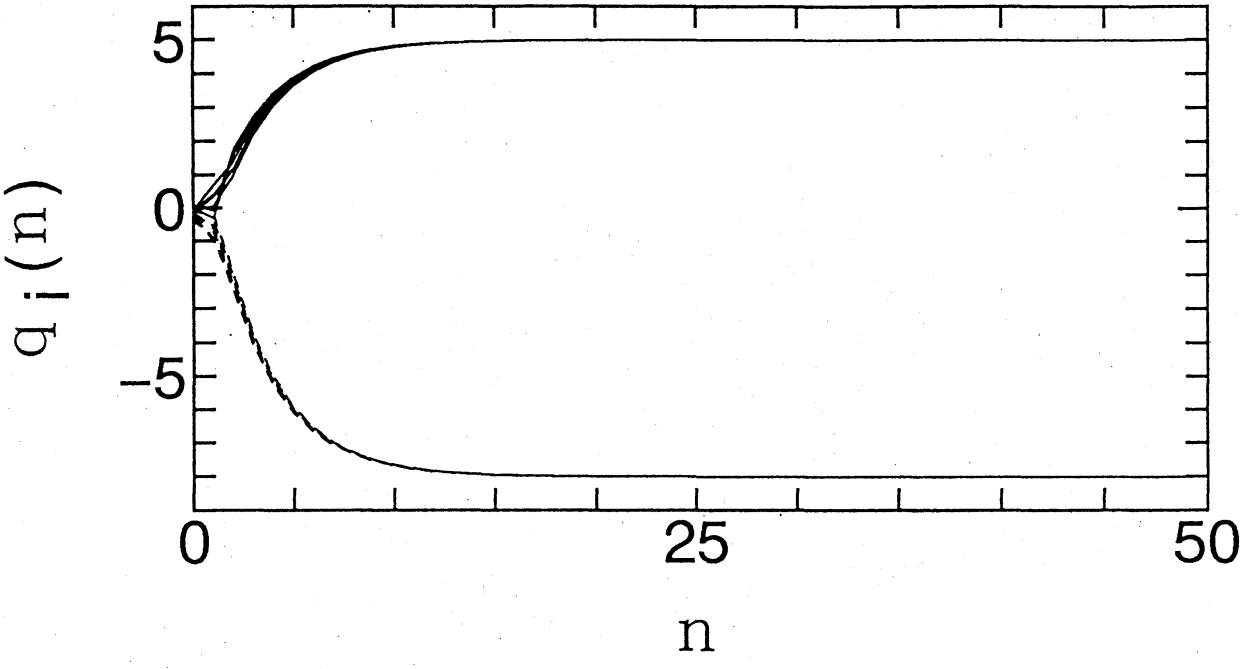

Nozawa Figure 7

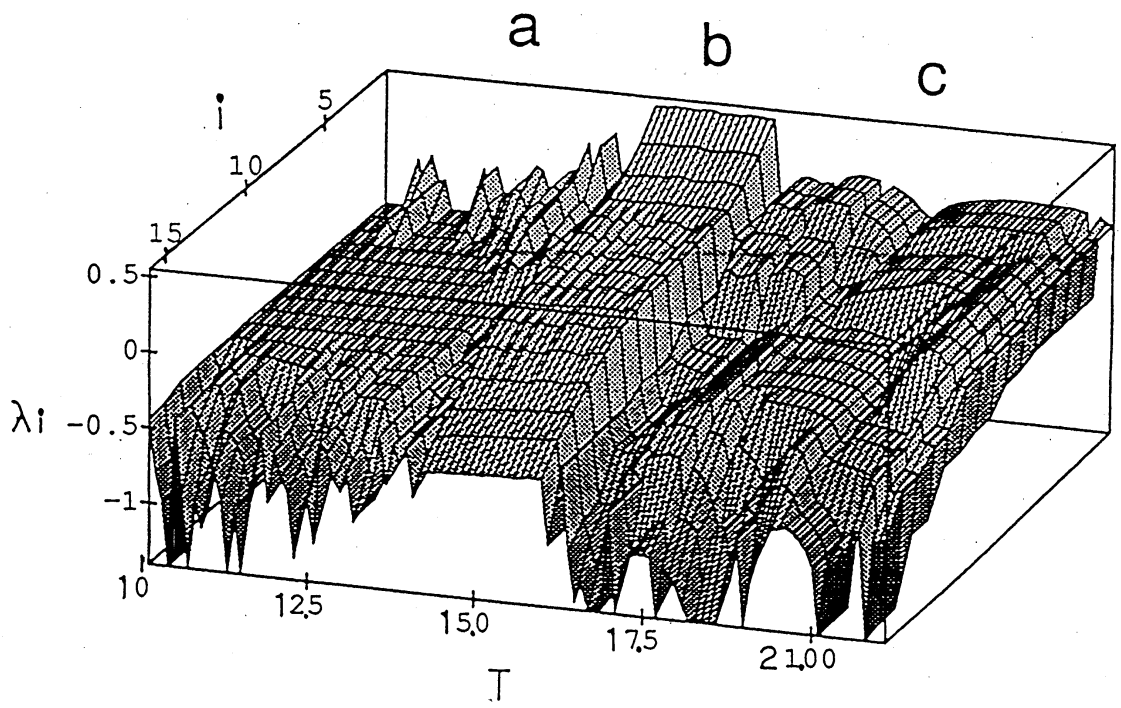

Nozawa Figure 8

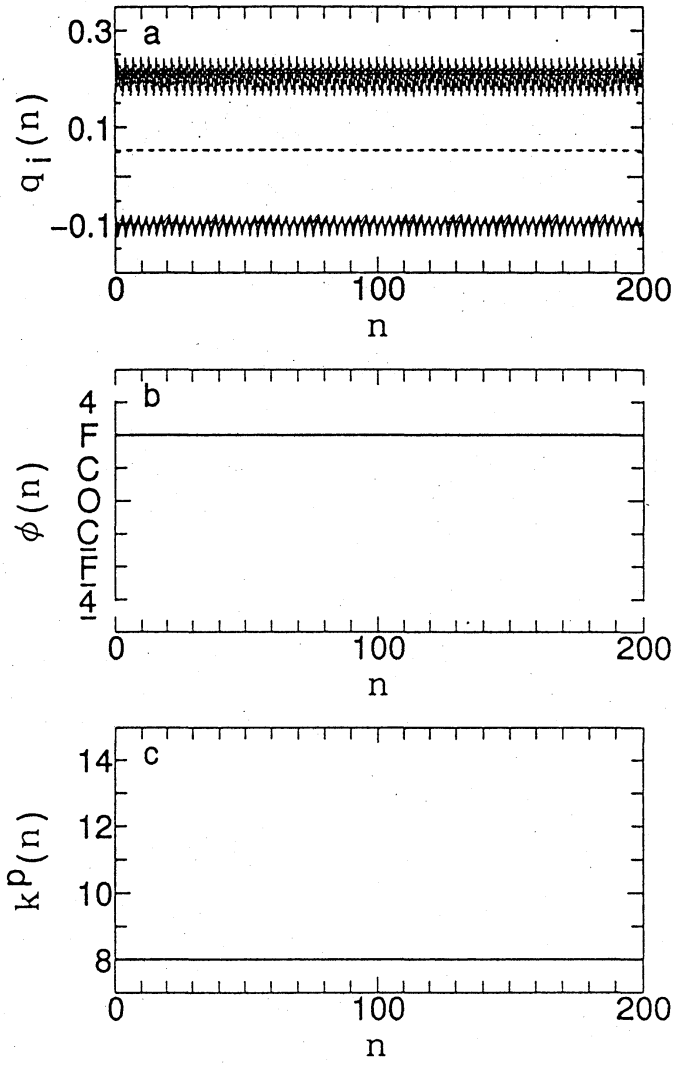

Nozawa Figure 9

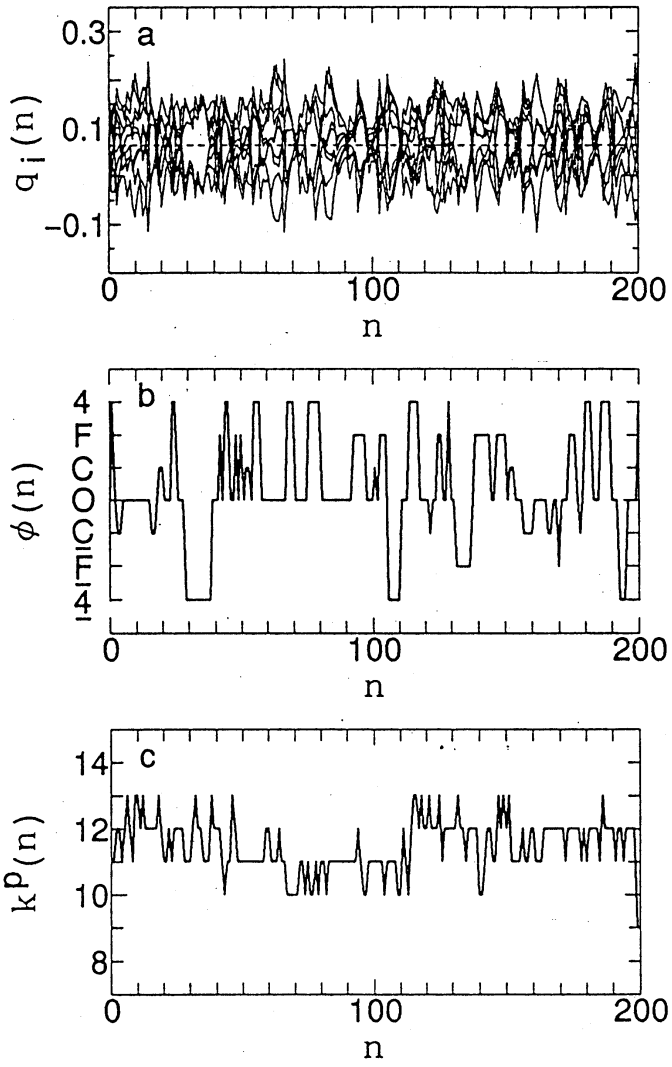

Nozawa Figure 10

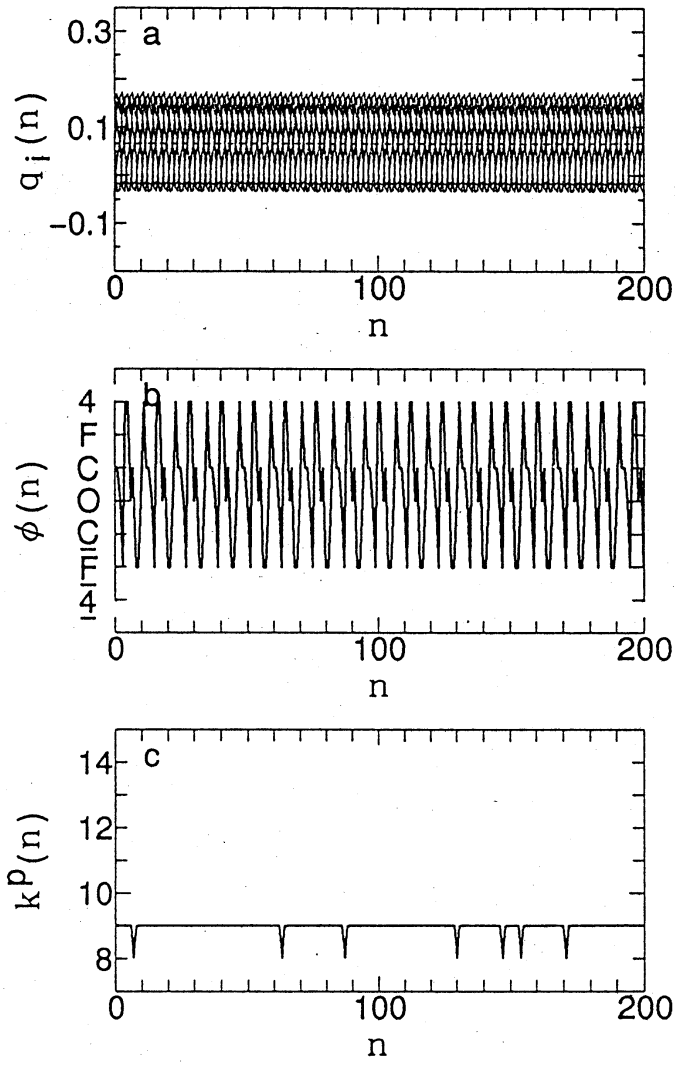

Nozawa Figure 11

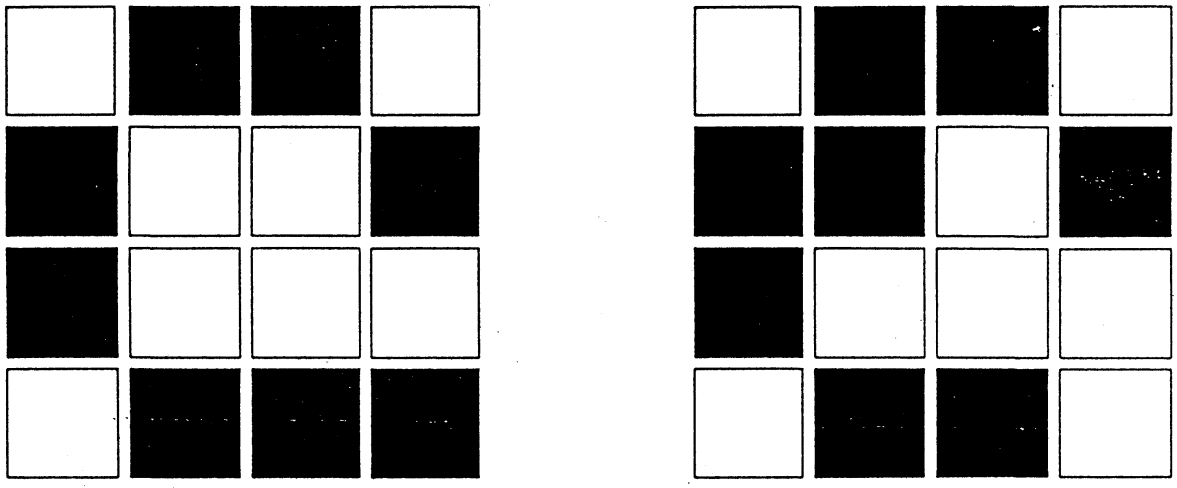

a b

Nozawa Figure 12

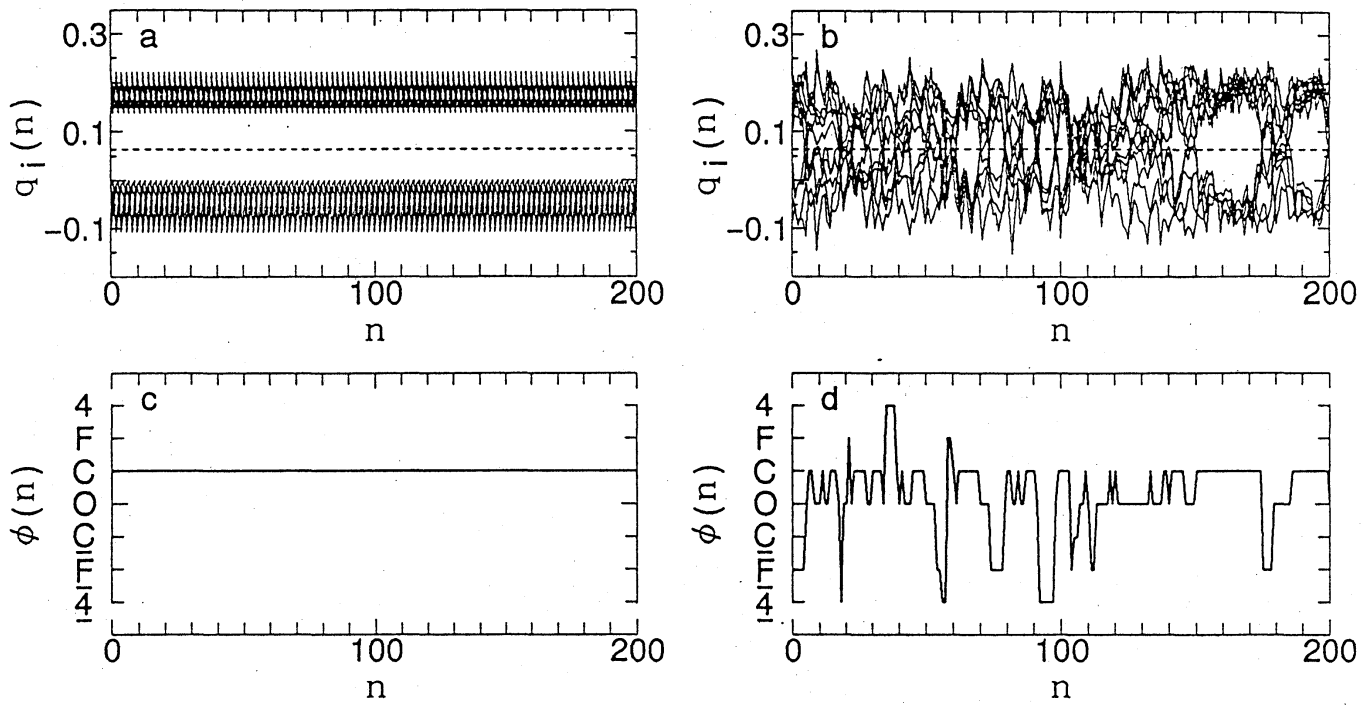

Nozawa Figure 13

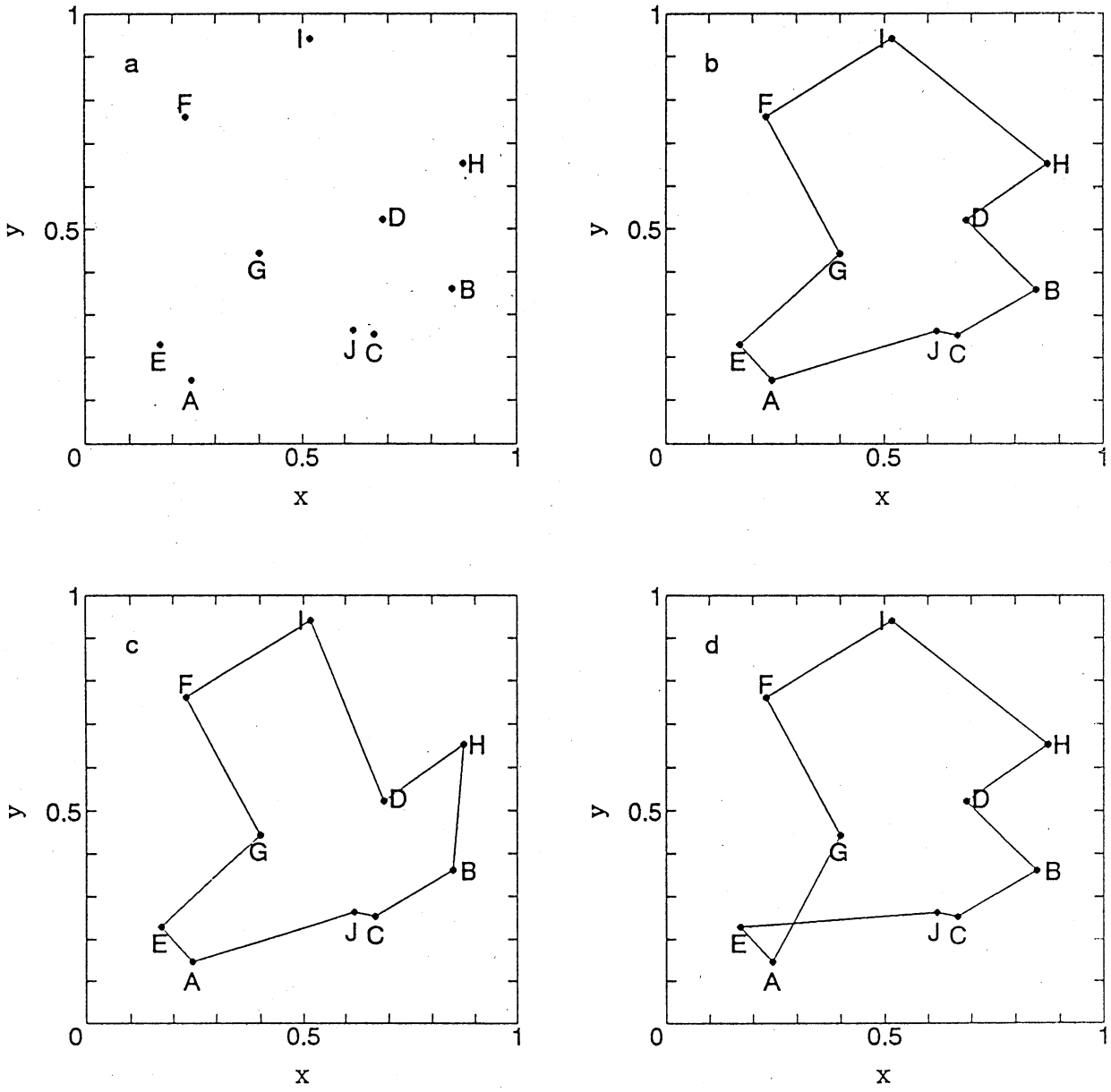

Nozawa Figure 14

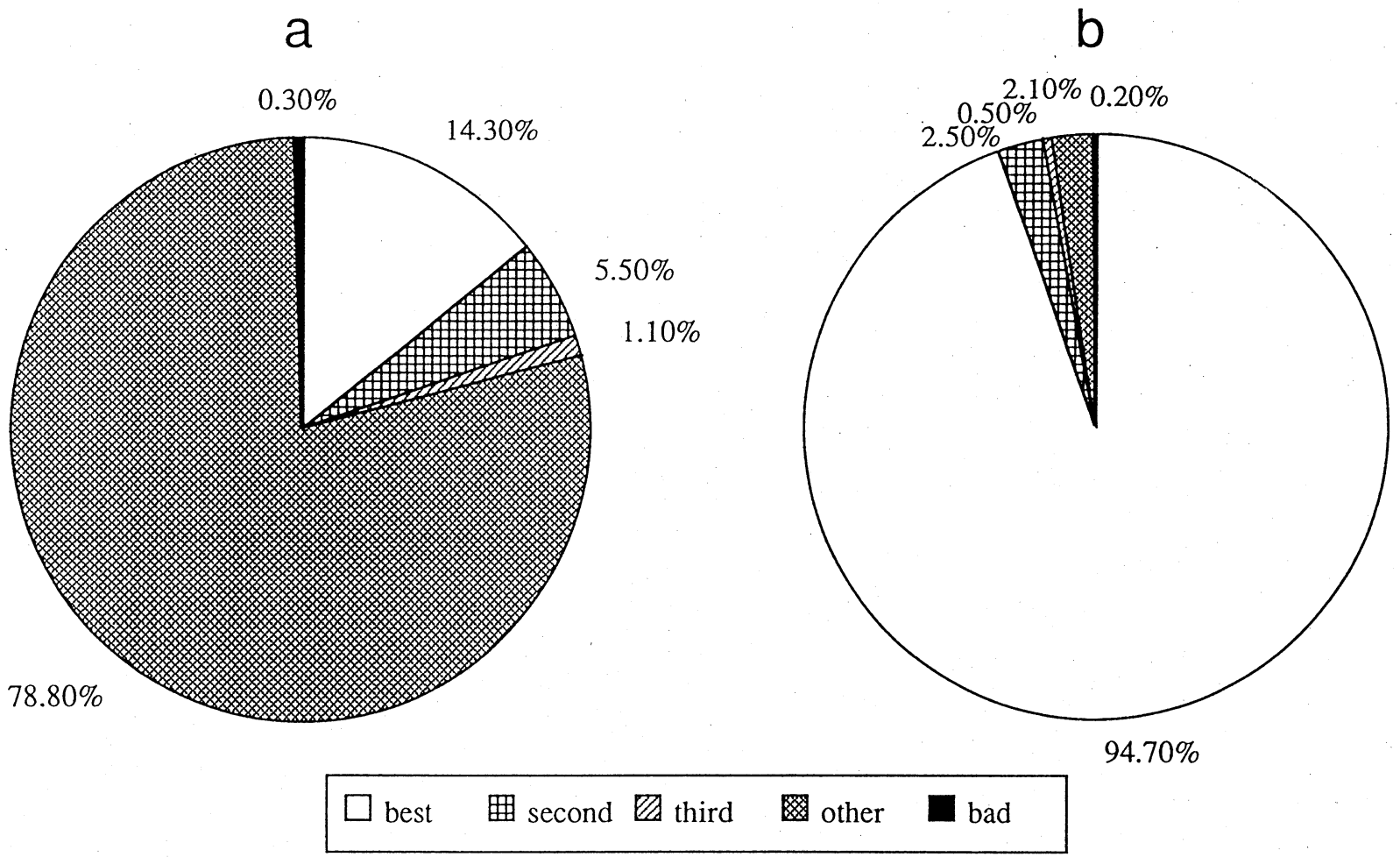

Nozawa Figure 15

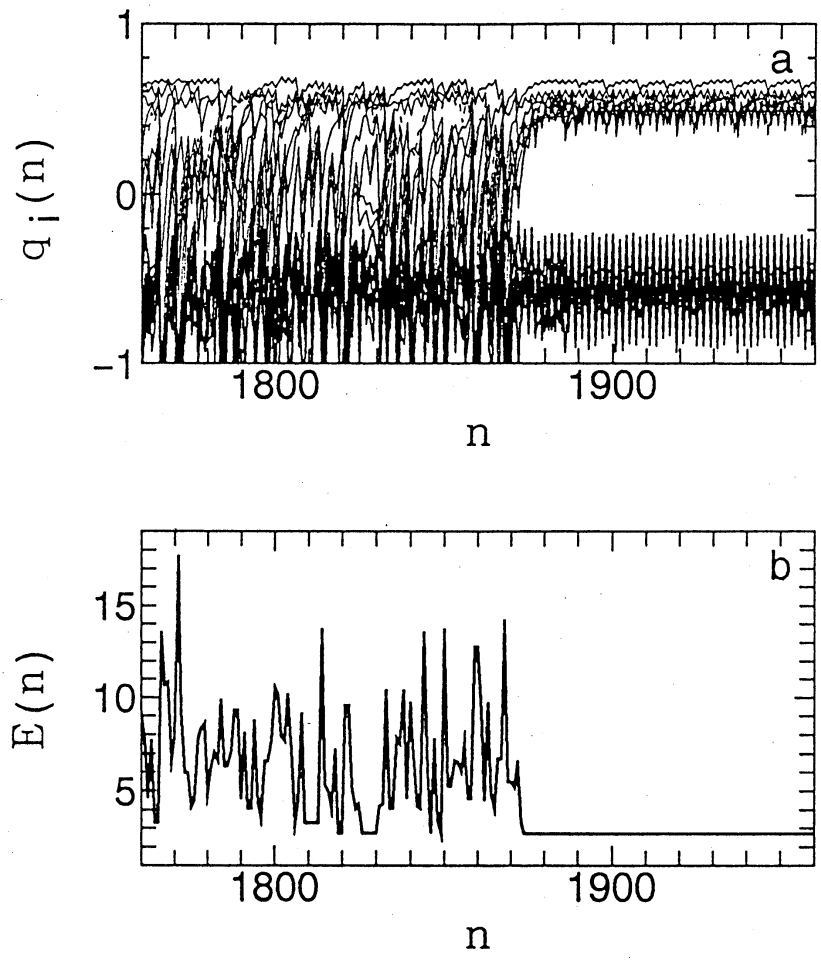

Nozawa Figure 16